# High throughput DNA sequencing with a microfabricated 96-lane capillary array electrophoresis bioprocessor

**Brian M. Paegel*, Charles A. Emrich†, Gary J. Wedemayer*, James R. Scherer*, and Richard A. Mathies*‡**

*Department of Chemistry and †Biophysics Graduate Group, University of California, Berkeley, CA 94720

Communicated by Alexander N. Glazer, University of California, Berkeley, CA, November 14, 2001 (received for review September 10, 2001)

**High throughput DNA sequencing has been performed by using a microfabricated 96-channel radial capillary array electrophoresis ($\mu$CAE) microchannel plate detected by a 4-color rotary confocal fluorescence scanner. The microchannel plate features a novel injector for uniform sieving matrix loading as well as high resolution, tapered turns that provide an effective separation length of 15.9 cm on a compact 150-mm diameter wafer. Expanded common buffer chambers for the cathode, anode, and waste reservoirs are used to simplify electrode addressing and to counteract buffering capacity depletion arising from the high electrophoretic current. DNA sequencing data from 95 successful lanes out of 96 lanes run in parallel were batch-processed with BASEFINDER, producing an average read length of 430 bp (phred q $\geq$ 20). Phred quality values were found to exceed 40 (0.01% probability of incorrectly calling a base) for over 80% of the read length. The $\mu$CAE system demonstrated here produces sequencing data at a rate of 1.7 kbp/min, a 5-fold increase over current commercial capillary array electrophoresis technology. Additionally, this system permits lower reagent volumes and lower sample concentrations, and it presents numerous possibilities for integrated sample preparation and handling. The unique capabilities of $\mu$CAE technology should make it the next generation, high performance DNA sequencing platform.**

Advances in DNA sequencing technologies over the past decade have been driven by the Human Genome Project (1). To achieve the ambitious goals of the genome project, sequencing centers replaced slab gel-based systems with capillary array electrophoresis (CAE) instruments that are based either on the scanning confocal detector developed in our laboratory (2, 3) or on sheath-flow detection (4, 5). Although the draft sequence of the human genome is now "complete" (6), expanded sequencing capacity is still required for the characterization of human sequence variation and for sequencing other genomes. In pursuing these goals, many technology development efforts are focused on the use of microfabricated electrophoretic analysis systems.

Microfabricated capillary electrophoresis devices were introduced by Manz and coworkers (7, 8) in the early 1990s. These microchips efficiently and very rapidly separated mixtures of fluorescent dyes and fluorescently labeled amino acids by using a fraction of the conventionally required capillary length. Initial experiments were rapidly followed by the demonstration of protocols for rapid DNA sizing and sequencing (9, 10), integrated thermal cycling fluidic circuitry (11), and clinically relevant genotyping (12). In subsequent work, the classical variables of DNA sequencing separations such as column length, sieving matrix composition, injection parameters, etc. have been explored and optimized (13, 14), producing read lengths as long as 800 bp for a 40-cm-long microfabricated capillary in 80 min (15).

Microfabricated capillary array electrophoresis ($\mu$CAE) devices are advantageous compared with drawn capillary array instrumentation because they allow monolithic array construction, precise definition of picoliter sample injection plugs, and the potential for integrated, low volume sample processing. Our group has pioneered the design and construction of microfabricated capillary array electrophoresis devices demonstrating rectilinear networks of 12 and 48 channels for parallel DNA fragment analysis (16, 17). The field was further advanced with the presentation of a 96-lane radial microchannel plate (MCP) layout together with a rotary confocal scanning detector and its use for high throughput genotyping (18).

The primary challenge in adapting the radial 96-lane MCP for DNA sequencing is attaining the necessary column lengths (13, 14). Folding channels to increase the effective separation length maintains a compact design compatible with modern wafer-scale fabrication. Although studies have shown that turns in folded channels can have a deleterious effect on electrophoretic separation quality (19, 20), we experimentally demonstrated with single-channel devices that low-dispersion, pinched turn geometries (hyperturns) circumvent this fundamental limitation (21).

We present here a new 96-channel radial $\mu$CAE MCP that exploits the advantages of microfabrication to perform high quality, high throughput DNA sequencing. The MCP incorporates optimized hyperturns to gain the effective separation length required for DNA sequencing while maintaining a compact, wafer-scale device. Furthermore, we have optimized the fluidic resistance of channels in the array for balanced sieving matrix loading. This DNA microprocessor has the performance characteristics required for the next generation of high speed DNA sequencing systems.

## Experimental Procedures

**Microdevice Fabrication and Design.** The microfabrication protocols for the 150-mm diameter substrates are similar to those previously described (17). Borofloat glass wafers (150 mm diameter; Schott, Yonkers, NY) were coated with a 2,000-Å film of silicon. A spin-coated film of photoresist (S1818, Shipley, Marlborough, MA) was exposed to UV light through a photomask in a contact printer. After developing, the pattern was transferred to the silicon film by reactive ion etching with $SF_6$ plasma. Formation of the channels was accomplished by isotropic wet chemical etching of the exposed glass in concentrated HF for ~4 min, resulting in a channel depth of ~30 $\mu$m. After etching, the photoresist was removed by oxygen plasma ashing. The 193 fluidic access ports (1.5-mm diameter) were diamond-drilled into the etched wafers by using a CNC mill. The wafers were then cleaned, and the remaining silicon was removed by reactive ion etching. The microchannels were enclosed by thermal compression bonding of a blank wafer to the etched and drilled channel plate. The finished microchannel network was coated according to a modified Hjerten procedure (22). Con-

Abbreviations: CAE, capillary array electrophoresis; MCP, microchannel plate.

‡To whom reprint requests and correspondence should be addressed. E-mail: rich@zinc.cchem.berkeley.edu.

The publication costs of this article were defrayed in part by page charge payment. This article must therefore be hereby marked "*advertisement*" in accordance with 18 U.S.C. §1734 solely to indicate this fact.

centric PMMA rings (3 mm high by 2 mm thick in cross section) defining large, common, moat-like 3-ml buffer reservoirs for the cathode and waste wells were affixed to the MCP with a silicone-based adhesive.

The layout of the 96-lane DNA sequencing MCP is presented in Fig. 1. The radial array of microchannels is organized around a central anode reservoir. Adjacent pairs of lanes are grouped into doublet structures that share common cathode and waste reservoirs. The arms of the injector are designed with different widths to balance the structure fluidically for even matrix loading to all access ports. The sample and waste arms are offset 250 $\mu$m to create an elongated plug-defining intersection with a volume of 1.2 nl. Each separation column is 200 $\mu$m wide, 30 $\mu$m deep, and is folded twice upon itself for an effective length of 15.9 cm by using four symmetrically tapered hyperturns with taper lengths of 100 $\mu$m and radii of curvature of 250 $\mu$m.

**Device Operation.** Before matrix loading, the separation channels and reservoirs at the cathode end of the array are filled with 1 $\times$ TTE buffer. The linear polyacrylamide sieving matrix is then forced in through the anode access port at 4,100 kPa for 5 min by using a high pressure loading system (23). Excess matrix is removed from the sample wells and 2 $\mu$l of sample introduced. The cathode and waste buffer moats are filled with 3 ml of 1 $\times$ TTE each. An elastomer buffer reservoir is affixed above the central anode access port and filled with 3 ml of 1 $\times$ TTE. The filled MCP is placed on a stage heated to 50°C on the 4-color confocal rotary scanner. An electrode ring array is placed over the chip to provide electrophoresis voltages to the various reservoirs. The electrode ring is fabricated with an embedded heater maintained at 60°C to prevent condensation of the buffer from the cathode and waste moats on the inner surfaces of the electrode array.

The sample is injected electrophoretically from the sample reservoir to the injection intersection at 500 V/cm for 60 s. During this period, the anode and cathode reservoirs are floated. The plug defined by the 250-$\mu$m intersection is driven down the separation column at 200 V/cm while a back-biasing electric field of 200 V/cm is applied at the sample and waste reservoirs to withdraw excess sample and prevent leakage from the reservoirs onto the column. These conditions are applied for 420 s. The separation electric field strength is then raised to 240 V/cm, and the sample and waste reservoirs are floated for the remainder of the analysis. Electrophoretic analysis is complete in 24 min. Following sequencing, the chip is purged of the sieving matrix by using the same high pressure loading device with a 4,100 kPa, 10-min water-flushing cycle. A single coating of the chip can be reused on average for 10 sequencing runs. The typical mode of failure is channel clogging, which is remedied by ashing at 500°C for 3 h and reapplying the Hjerten coating.

**Data Acquisition and Reduction.** The Berkeley 4-color rotary scanner has been described in detail (18). A conceptual schematic of the system is presented in Fig. 2. Briefly, excitation at 488 nm from an argon ion laser is coupled into the optical path with a dichroic beam splitter. The laser light is passed through the hollow shaft of a stepper motor, displaced from the rotation axis by 1-cm with a rhomb prism, and focused on the microchannels of the electrophoresis MCP through a 20$\times$ objective. Fluorescence is collected by the objective and passed back through the hollow shaft and dichroic beam splitter and sorted into four spectral channels. Data acquisition is synchronized with a slit flywheel attached to the rotor and monitored with a photodiode. The scanning objective is focused on the matrix-filled microchannels by monitoring the water Raman scattering in the 580-nm channel. Raman scattering is also used to define the locations of the lanes for data acquisition. After electrophoretic analysis, the 4-color electropherograms are used as input for the

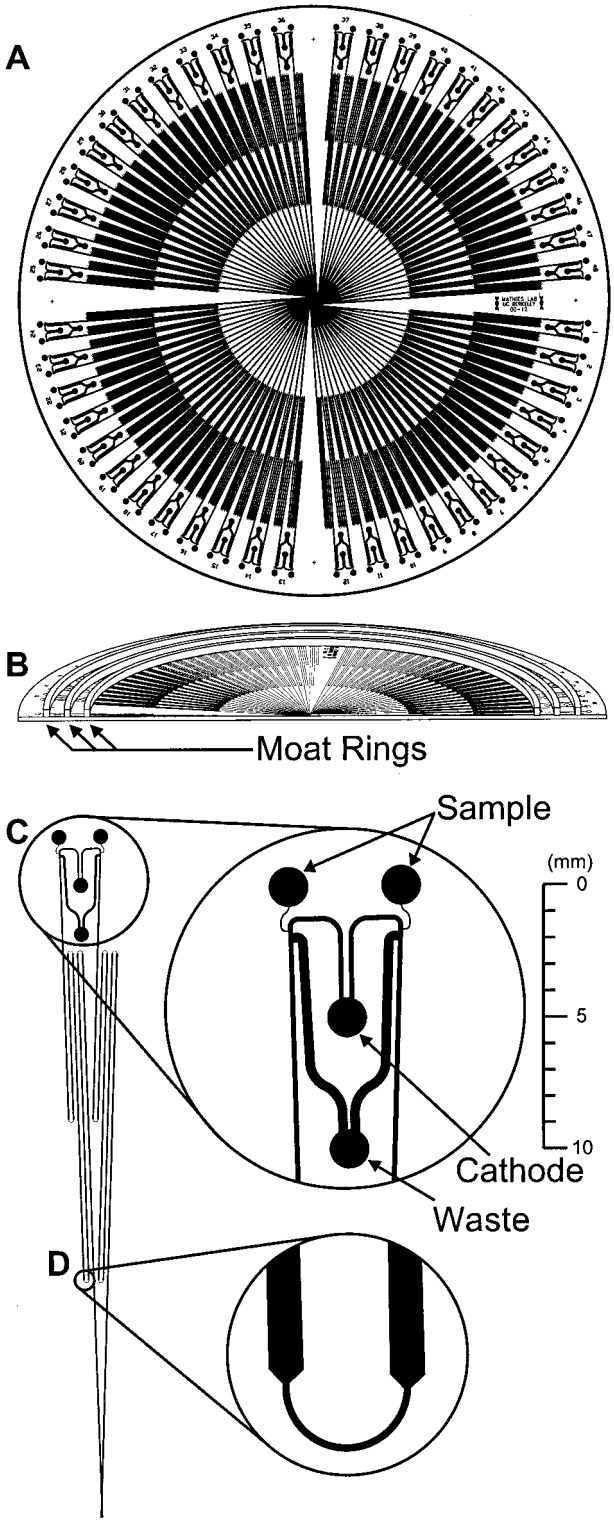


**Fig. 1.** (*A*) Overall layout of the 96-lane DNA sequencing microchannel plate (MCP). (*B*) Vertical cut-away of the MCP. The concentric PMMA rings formed two electrically isolated buffer moats that lie above the drilled cathode and waste ports. (*C*) Expanded view of the injector. Each doublet features two sample reservoirs and common cathode and waste reservoirs. The arm from the sample to the separation channel is 85 $\mu$m wide, and the arm from the waste to the separation channel is 300 $\mu$m wide. The separation channel connecting the central anode and cathode is 200 $\mu$m wide. (*D*) Expanded view of the hyperturn region. The turns are symmetrically tapered with a tapering length of 100 $\mu$m, a turn channel width of 65 $\mu$m, and a radius of curvature of 250 $\mu$m. Channel widths and lengths are not drawn to scale.

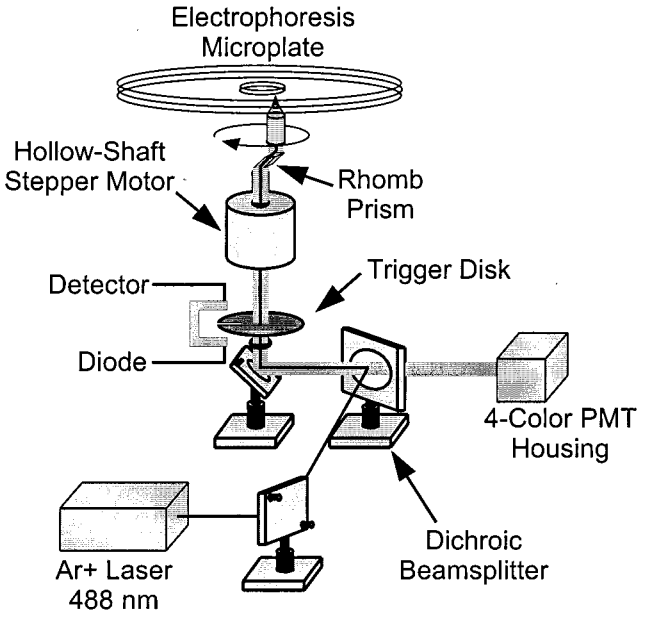


**Fig. 2.** The Berkeley 4-color rotary confocal scanner. Excitation at 488 nm from an argon ion laser is passed through the hollow shaft of a stepper motor. The beam is displaced to a radius of 1 cm and passed through a 20× objective. Fluorescence (gray line) is collected by the objective and passed through the dichroic beam splitter to the 4-color detection system.

base calling software BASEFINDER (24). For presentation, the BASEFINDER output is used to generate a sequencing gel image of the 96-electropherogram data. Processed, uncalled output from BASEFINDER is fed to the base-calling program PHRED (25) to obtain phred quality values.

**Sample and Matrix Preparation.** Single-stranded DNA sequencing samples labeled with energy-transfer primers were obtained from Amersham Biosciences. The 2-ml sample was resuspended in a 70% deionized formamide solution in distilled, deionized water to a volume of 4 ml (0.5× according to manufacturer protocols). Linear polyacrylamide was synthesized according to described protocols with several modifications (26). Briefly, 10 ml of 4.5% wt/vol acrylamide monomer (electrophoresis grade), 1 × TTE (50 mM Tris base/50 mM TAPS acid/1 mM EDTA, pH 8.3), and 7 M urea solution was sparged with helium for 2 h. Polymerization was initiated by adding sequentially 3 $\mu$l of 10% (wt/vol) ammonium persulfate and 3 $\mu$l of 10% (vol/vol) *N*,*N*,*N*′,*N*′-tetramethylethylenediamine. Both initiator solutions were prepared in distilled, deionized water. The sparging line was raised from the solution, and helium flowed over the surface of the polymerizing solution for 1 h. The line was then removed from the polymerizing vial leaving a positive pressure of helium, and the polymerization was allowed to proceed overnight. All degassing and synthesis steps were carried out at 4°C. Molecular weight and polydispersity analysis of the acrylamide sieving matrix was performed by Impact Analytical (Midland, MI).

## Results and Discussion

Fig. 3 presents the results of a 96-lane sequencing run on M13mp18 sequencing vector DNA by using the M13 (−40) energy-transfer labeled forward sequencing primer in which the same sample is run in each lane. The data are presented in a sequencing gel format with each band representing one sequenced base; the bases are color-coded blue for cytosine, green for adenine, black for guanine, and red for thymine. Of the 96 channels presented, only channel 72 failed to produce sequencing data because of a defect in photolithography. The image contains 41 kb sequenced to >99% accuracy in the 16-min sequencing window, a net sequencing capacity of 1.7 kbp/min. Lane-to-lane variance in mobility is attributed to electrode placement as well as variability in coating and gel filling.

Fig. 4 presents expanded views of BASEFINDER-processed traces from the start, middle, and end of a lane of *average* performance (427 phred 20 bases called). The first peaks exhibited lower intensity because the concentration of the smaller fragments was lower. A problematic compression sequence CCCCGGG at base position 43 was well resolved and called correctly. The middle region, which extended on average 350 bases over 95 lanes, reproducibly exhibited baseline-resolved processed data. The end region of this stretch of M13 sequence contains several homopolymeric series that were typically undercalled by BASEFINDER.

The average phred quality value (10-base window average) for the 95 successful channels as a function of base position is presented in Fig. 5. Phred quality values are the widely accepted convention used to express the probability of miscalling a peak based on key parameters such as resolution, spectral cross talk, and uniformity of peak spacing. The quality values, $q$, are logarithmically proportional to the probability of miscalling an identified peak in the chromatogram, $P_{err}$, by the relation $P_{err} = 10^{-q/10}$. Phred 20, or an accuracy of 99%, has been identified as the minimal acceptable value for sequencing data. Sequencing read length may be defined as the total number of bases called with phred $q > 20$. By this criterion, our 95-lane average read length on the microchip is 430 bp. We were typically able to produce greater than phred 20 within 10 called bases. Phred quality value distributions at 10, 100, 200, 300, 400, and 450 called bases illustrate the high lane-to-lane precision of the instrument. At base position 10, there is a bimodal distribution of scores where some lanes have sequenced through the initial 10-bp window of lower quality, whereas others are just reaching the end of the primer peak. Base positions 100, 200, and 300 demonstrate excellent average quality values and tight distributions indicative of good lane-to-lane consistency. Two outlying lanes having read lengths of 187 and 257 bp are evidenced by the two lower quality bins in the base positions 200 and 300 distributions. The distributions at 400 and 450 bp are much broader and lower in average quality, consistent with our standard deviation of the distribution of read lengths (as defined previously) of ±30 bp.

High density capillary array electrophoresis sequencing poses new challenges that are absent in single-channel demonstration experiments. In the classical microchip DNA fragment-sizing experiment (9), platinum electrodes are immersed directly into the 1-mm diameter, ~2-$\mu$l drilled wells, and electrophoretic analyses are performed. When this methodology was applied to single-channel DNA sequencing experiments that require longer electrophoresis times and higher currents, we noticed irreproducibility in read length and electrophoretic mobility as well as difficulty in maintaining 2-$\mu$l aqueous buffer volumes at elevated temperatures. In subsequent single-channel optimization experiments, the volumes of the cathode and anode buffer wells were increased to 50 $\mu$l, and an increase in read length and reproducibility as well as increased electrophoretic current stability were observed. This observation indicated that the buffering capacity of the small volume reservoirs was insufficient.

The effect of electrophoresis on the chemical composition of the buffer wells making electrical contact with the cathode and anode electrodes and its significance for reproducibility in the limit of smaller well volumes has been discussed by Bello (27). It is essential to maintain buffering of electrolytically generated protons and hydroxyls through the entire analysis because the phosphodiester backbone of DNA is susceptible to protonation and subsequent mobility shift. Assuming the measured electrophoretic current of 3 mA resulted totally in electrolysis of water,

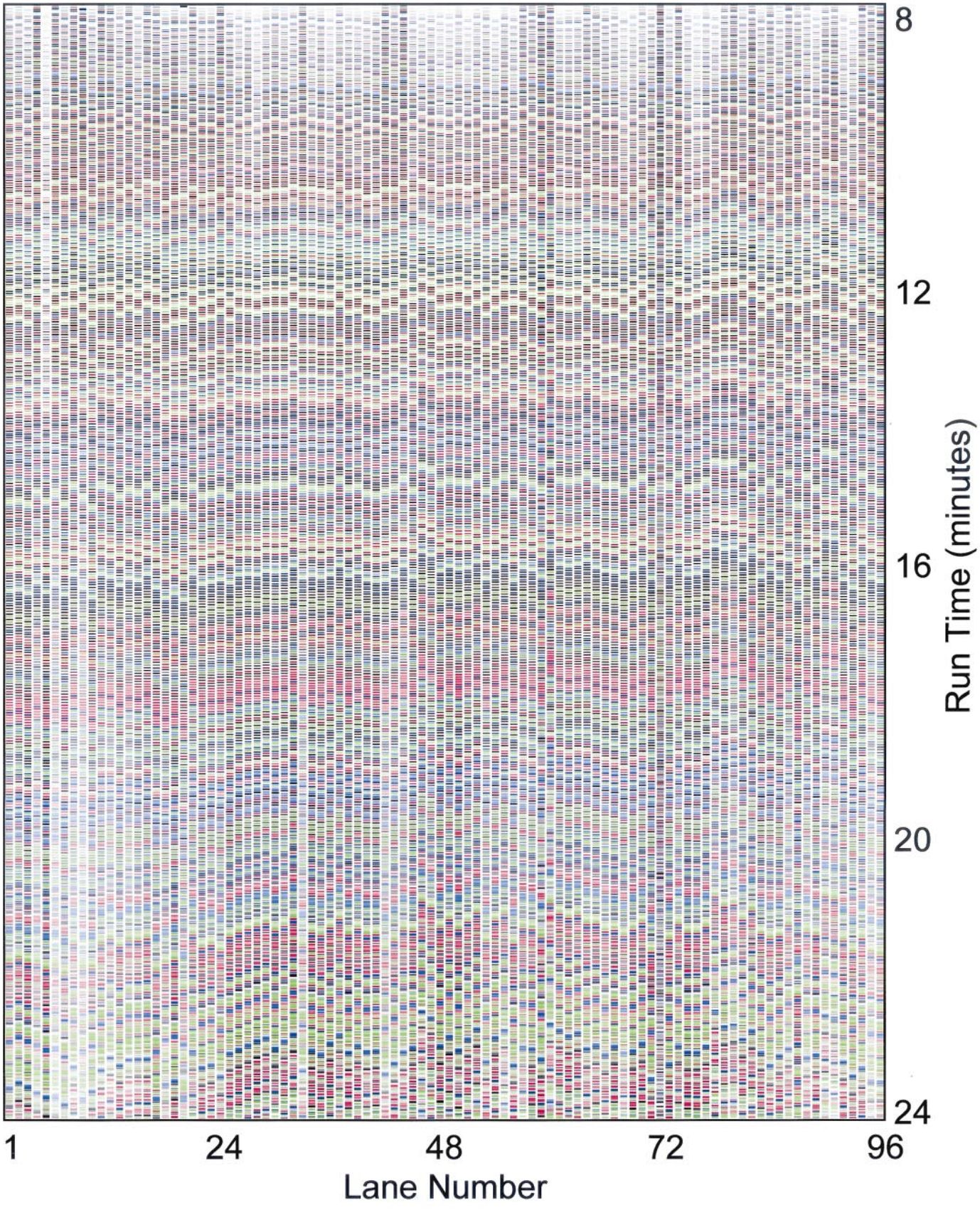


**Fig. 3.** Image of processed sequencing data from the 96-lane DNA sequencing microdevice. Each band in a lane represents one base. The DNA bases C, A, G, and T are color coded as blue, green, black, and red, respectively. The data for all lanes were collected in 24 min after injection; 4.5% wt/vol linear polyacrylamide, 50°C, energy-transfer labeled M13mp18 forward sequencing primer.

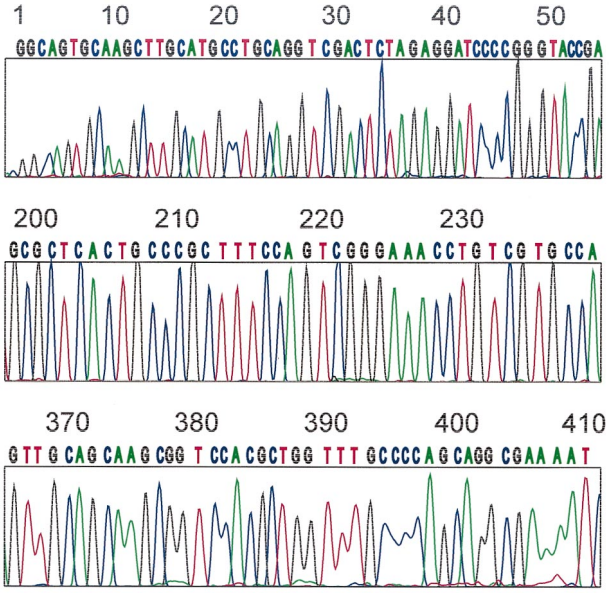


**Fig. 4.** Processed sequencing output from a lane in Fig. 3 exhibiting *average* performance. The three panels display the typical quality of data obtained at the start, middle, and end of the run. Base numbers are indicated above the base calls.

a $H^+$ production rate of $3 \times 10^{-8}$ mol/s is calculated. Given 0.05 M Tris base present in the 1 × TTE buffer system, a buffer well volume of 2 $\mu$l would be titrated in 0.3 s. A well volume of 3 ml as used in this experiment would be titrated in 83 min of electrophoresis. However, this value assumes that the entire well volume is accessible to protons as they are generated at the anode. Realistically, we must take into account proton advection and diffusion when determining the total volume available for buffering. A model based on the free-solution proton mobility (28) suggests that placing the electrode directly above the central anode hole in the 3-ml reservoir still leads to a titration time of 9 s. By adopting a circularly shaped electrode and immersing the electrode distal to the central anode hole in the reservoir, the entire volume of the reservoir is used, and stable current is observed over the course of the entire run.

Matrix filling presents an additional important, practical challenge. Because the sample arms are typically much shorter than either the cathode or waste, pressure filling from the anode preferentially charged the sample arm and overflowed the sample access ports before the channels to the cathode and waste were filled with matrix. Reservoirs that are overflowed with matrix are difficult to clean out and complicate robotic sample loading. We chose to modulate the relative fluidic resistances of these channels to balance matrix flow during loading. Polyacrylamide solutions exhibit highly non-Newtonian, shear-thinning behavior, and thus it was necessary to balance fluid flow empirically. The balanced channel widths are 85, 200, and 300 $\mu$m for the sample, cathode, and waste arms, respectively. The present device was loaded evenly with matrix to all access ports in 5 min. This fluid-balanced injector also exhibits beneficial electrophoretic properties because the difference in channel widths between the sample and waste arms establishes a conductivity differential. Application of an injection potential between the sample and waste results in one-half of the applied potential being dropped on the sample arm (vs. one-fifth if the arms were the same width). We may therefore create high electric fields in the sample arm with only modest potentials. This is important for high density arrays in which wells may be

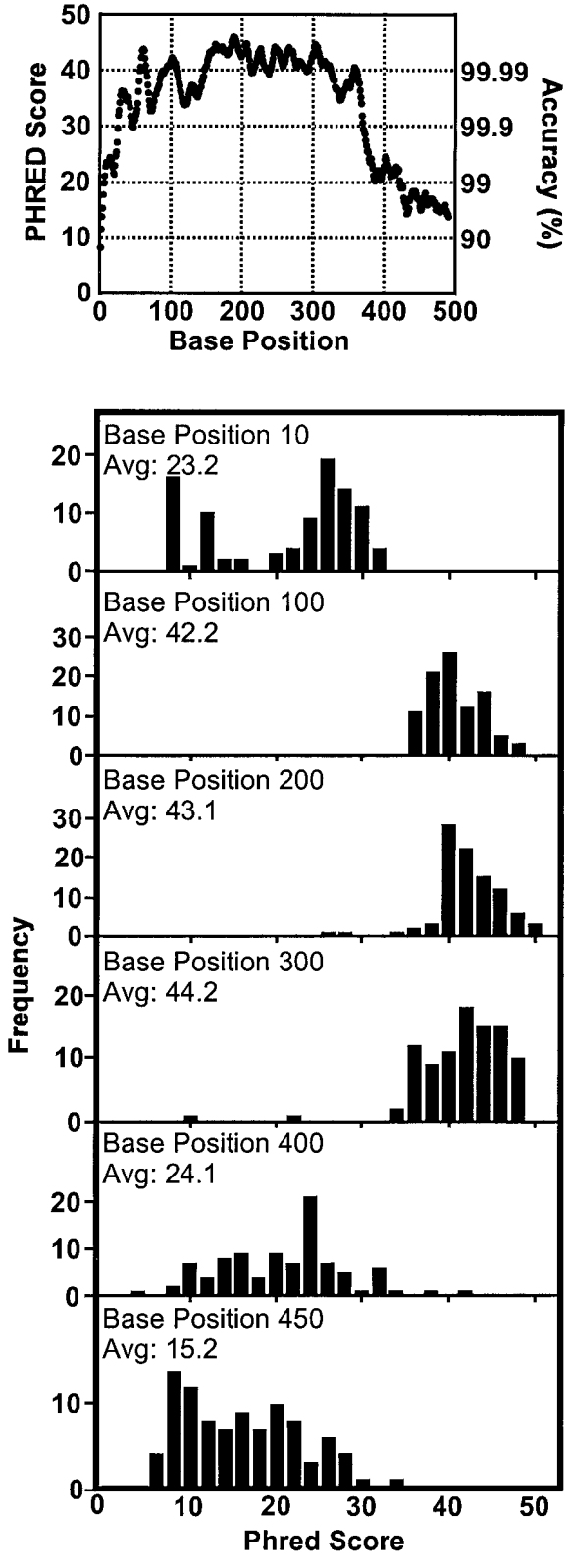


**Fig. 5.** The average phred score over the 95 passed lanes as a function of base position (*Upper*). Miscall probabilities are listed at the right as accuracy. The distribution of phred scores from the 95 passed lanes is shown at six positions in the processed data (*Lower*). The base position and average score of each distribution is listed above the graphs. Distributions representing the beginning (10 bp), high quality (100, 200, and 300 bp), declining quality (400 bp), and end (450 bp) regions of the separation are shown.

spaced very close together and air breakdown limits the user to ~1 kV/cm.

A rigorous optimization of system parameters is expected to yield enhanced read lengths. Matrix composition is the most significant of these remaining variables. Size-exclusion chromatography of the linear polyacrylamide matrix used in these experiments yielded results consistent with its DNA sequencing performance. The polymer was found to contain a bimodal distribution of molecular weights divided evenly between a peak centered at ~200 kDa and another centered at ~4.5 MDa. Increasing the weight average molecular weight of the linear polyacrylamide sieving from 500 kDa to 10–17 MDa, as well as spiking the high molecular weight matrix with a small percentage of low molecular weight polymer (approximately 300 kDa), results in increased separation performance (29). We conclude that the primary reason for the read length limit of 430 bp observed here is the particular polymer used in these initial experiments. Experiments on real-world sequencing samples with improved polymer matrices are in progress.

## Conclusions and Prospects

We have developed a 96-channel $\mu$CAE system and used it to perform the first high throughput DNA sequencing on a microfabricated device. A sequencing rate of ~30 bp/s is achieved with an order of magnitude reduction in electrophoresis time compared with commercial CAE systems. When coupled with automated matrix filling, sample loading, device cleaning, and data analysis methods that we have developed, this system has the capabilities needed for the next generation of DNA sequencing technology. The enhanced throughput of $\mu$CAE with its potential for integrated sample preparation, handling, and purification should make the bioanalytical paradigm shift to $\mu$CAE even greater in scope and significance than the transition from slab gels to capillary arrays.

Microfabrication was carried out at the University of California Berkeley Microfabrication Laboratory. This research was supported by grants from the National Institutes of Health (HG01399) and from the Director, Office of Science, Office of Biological and Environmental Research of the U. S. Department of Energy under Contract DEFG91ER61125. Additional support was provided by Amersham Biosciences. B.M.P. was supported by a National Human Genome Research Institute, National Institutes of Health trainee fellowship from the Berkeley Program in Genomics (T32 HG00047).

1. Collins, F. S., Patrinos, A., Jordan, E., Chakravarti, A., Gesteland, R., Walters, L., Fearon, E., Hartwelt, L., Langley, C. H., Mathies, R. A., *et al.* (1998) *Science* **282,** 682–689.
2. Mathies, R. A. & Huang, X. C. (1992) *Nature (London)* **359,** 167–169.
3. Kheterpal, I., Scherer, J. R., Clark, S. M., Radhakrishnan, A., Ju, J. Y., Ginther, C. L., Sensabaugh, G. F. & Mathies, R. A. (1996) *Electrophoresis* **17,** 1852–1859.
4. Kambara, H. & Takahashi, S. (1993) *Nature (London)* **361,** 565–566.
5. Crabtree, H. J., Bay, S. J., Lewis, D. F., Zhang, J. Z., Coulson, L. D., Fitzpatrick, G. A., Delinger, S. L., Harrison, D. J. & Dovichi, N. J. (2000) *Electrophoresis* **21,** 1329–1335.
6. Lander, E. S., Linton, L. M., Birren, B., Nusbaum, C., Zody, M. C., Baldwin, J., Devon, K., Dewar, K., Doyle, M., FitzHugh, W., *et al.* (2001) *Nature (London)* **409,** 860–921.
7. Manz, A., Graber, N. & Widmer, H. M. (1990) *Sens. Actuator B-Chem.* **1,** 244–248.
8. Harrison, D. J., Fluri, K., Seiler, K., Fan, Z. H., Effenhauser, C. S. & Manz, A. (1993) *Science* **261,** 895–897.
9. Woolley, A. T. & Mathies, R. A. (1994) *Proc. Natl. Acad. Sci. USA* **91,** 11348–11352.
10. Woolley, A. T. & Mathies, R. A. (1995) *Anal. Chem.* **67,** 3676–3680.
11. Woolley, A. T., Hadley, D., Landre, P., deMello, A. J., Mathies, R. A. & Northrup, M. A. (1996) *Anal. Chem.* **68,** 4081–4086.
12. Tian, H. J., Brody, L. C., Fan, S. J., Huang, Z. L. & Landers, J. P. (2001) *Clin. Chem.* **47,** 173–185.
13. Schmalzing, D., Adourian, A., Koutny, L., Ziagura, L., Matsudaira, P. & Ehrlich, D. (1998) *Anal. Chem.* **70,** 2303–2310.
14. Liu, S. R., Shi, Y. N., Ja, W. W. & Mathies, R. A. (1999) *Anal. Chem.* **71,** 566–573.
15. Koutny, L., Schmalzing, D., Salas-Solano, O., El-Difrawy, S., Adourian, A., Buonocore, S., Abbey, K., McEwan, P., Matsudaira, P. & Ehrlich, D. (2000) *Anal. Chem.* **72,** 3388–3391.
16. Woolley, A. T., Sensabaugh, G. F. & Mathies, R. A. (1997) *Anal. Chem.* **69,** 2181–2186.
17. Simpson, P. C., Roach, D., Woolley, A. T., Thorsen, T., Johnston, R., Sensabaugh, G. F. & Mathies, R. A. (1998) *Proc. Natl. Acad. Sci. USA* **95,** 2256–2261.
18. Shi, Y. N., Simpson, P. C., Scherer, J. R., Wexler, D., Skibola, C., Smith, M. T. & Mathies, R. A. (1999) *Anal. Chem.* **71,** 5354–5361.
19. Jacobson, S. C., Hergenroder, R., Koutny, L. B., Warmack, R. J. & Ramsey, J. M. (1994) *Anal. Chem.* **66,** 1107–1113.
20. Culbertson, C. T., Jacobson, S. C. & Ramsey, J. M. (1998) *Anal. Chem.* **70,** 3781–3789.
21. Paegel, B. M., Hutt, L. D., Simpson, P. C. & Mathies, R. A. (2000) *Anal. Chem.* **72,** 3030–3037.
22. Hjerten, S. (1985) *J. Chromatogr.* **347,** 191–198.
23. Scherer, J. R., Paegel, B. M., Wedemayer, G. J., Emrich, C. A., Lo, J., Medintz, I. L. & Mathies, R. A. (2001) *BioTechniques* **31,** 1150–1156.
24. Giddings, M. C., Severin, J., Westphall, M., Wu, J. Z. & Smith, L. M. (1998) *Genome Res.* **8,** 644–665.
25. Ewing, B. & Green, P. (1998) *Genome Res.* **8,** 186–194.
26. Ruiz-Martinez, M. C., Berka, J., Belenkii, A., Foret, F., Miller, A. W. & Karger, B. L. (1993) *Anal. Chem.* **65,** 2851–2858.
27. Bello, M. S. (1996) *J. Chromatogr. A* **744,** 81–91.
28. Atkins, P. (1994) *Physical Chemistry* (Freeman, New York).
29. Zhou, H. H., Miller, A. W., Sosic, Z., Buchholz, B., Barron, A. E., Kotler, L. & Karger, B. L. (2000) *Anal. Chem.* **72,** 1045–1052.